POLITECNICO DI TORINO
Repository ISTITUZIONALE

Quadratic Form-Based Spectrum Sensing Algorithm for 6G Cognitive Radio Networks

Original
Quadratic Form-Based Spectrum Sensing Algorithm for 6G Cognitive Radio Networks / Alfano, G., Riviello, D.G., Garello, R.. - (2025), pp. 1-6. (2025 IEEE Wireless Communications and Networking Conference, WCNC 2025 Milano (Ita) 24 - 27 March 2025) [10.1109/wcnc61545.2025.10978141].

Availability:
This version is available at: 11583/3001962 since: 2025-07-19T16:18:06Z

Publisher:
IEEE

Published
DOI:10.1109/wcnc61545.2025.10978141

Terms of use:

This article is made available under terms and conditions as specified in the corresponding bibliographic description in the repository

Publisher copyright
IEEE postprint/Author's Accepted Manuscript

©2025 IEEE. Personal use of this material is permitted. Permission from IEEE must be obtained for all other uses, in any current or future media, including reprinting/republishing this material for advertising or promotional purposes, creating new collecting works, for resale or lists, or reuse of any copyrighted component of this work in other works.

(Article begins on next page)

28 June 2026

Quadratic Form-Based Spectrum Sensing Algorithm for 6G Cognitive Radio Networks

Giusi Alfano*, Daniel Gaetano Riviello†, Roberto Garello*
*Department of Electronics and Telecommunications (DET), Politecnico di Torino, Torino, Italy
†CNR-IEIIT, Consiglio Nazionale delle Ricerche, Torino, Italy
Email: d020860@polito.it, daniel.riviello@cnr.it, roberto.garello@polito.it

***Abstract*—Spectrum Sensing will play a pivotal role in 6G Cognitive Radio Networks, in which unlicensed users could dynamically use the spectrum and perform opportunistic transmission. In this paper, we focus on a multiple-antenna data-aided Spectrum Sensing algorithm and we compute the exact Moment Generating Function and probability density function under the null hypothesis of such test statistic, by resorting to tools from finite-dimensional random matrix theory. The test at hand is formulated in terms of a quadratic form with unit-norm random vector and random kernel matrix with determinantal joint probability distribution of its eigenvalues. The algorithm exploits the availability of a set of auxiliary data, collected under the assumption of primary signal presence. Results, presented in terms of Receiver Operating Characteristic curve and detection probability vs. the Signal-to-Noise Ratio, show that the presented test outperforms some well-established sensing schemes, such as the Generalized Likelihood Ratio Test and the Roy's Largest Root Test. Furthermore, we compare the outcomes of our analytical derivation with corresponding Monte Carlo simulated data in scenarios with both spatio-temporally uncorrelated and correlated samples.**

***Index Terms*—spectrum sensing, quadratic form, multi-antenna, random matrix theory, cognitive radios, 6G**

I. Introduction

The next generation of mobile network standards for cellular technology, 6G, foresees the coexistence of several wireless communication systems as *self-regulating societies of mobile radios* [1]. In view of the forthcoming integration of terrestrial and satellite networks as well [2], [3], spectrum sharing capabilities are among the most desirable features of wireless networked systems [4]. In this context, 6G Cognitive Radios Networks (CRN) are expected to play a massive role by enhancing spectrum utilization and by facilitating the coexistence between unlicensed and licensed networks [4]. A fundamental task of CRN is the ability of discriminating the presence of a primary user/signal (busy channel) against background noise (clear channel).

Spectrum Sensing (SS) plays, indeed, a major role in resource sharing, and the investigation of efficient sensing strategies has been one of the main goals of the wireless communications community during the last two decades [5]–[7]. Our focus is on eigenvalue-based spectrum sensing strategies, mostly devised by exploiting features of (linear) spectral statistics (see e.g., [8]–[10], and [11, and references therein]) of a random matrix of properly arranged signal samples, collected across a given spatio/temporal sensing range. Test statistics are, in turn, computed by following classical approaches of estimation theory (e.g., resorting to Likelihood Ratio based criteria [12]), or adopting heuristics, as in the algorithm at the core of our work.

In this paper, we focus hereinafter on a secondary-data aided spectrum sensing scheme, introduced in [13], and subsequently thoroughly analyzed in [14], where numerical tests showed it to outperform conventional schemes like those based on the Generalized Likelihood Ratio Test (GLRT) [12] or on the classical Roy's Largest Root Test [15], [16].

Analytical performance analysis of the test at hand calls for the characterization of a quadratic form in the eigenvalues of the Hermitian random matrix representing the collected data covariance. Interestingly, statistics of such a quadratic form can be exactly computed in terms of its Moment Generating Function (MGF), under the null assumption of the sensing test (i.e., under hypothesis of primary signal absence), in two relevant scenarios, namely when collected data samples are spatio-temporally uncorrelated, and, in turn, when spatial correlation between the antennas placed at the sensing unit is present. Upon Laplace inversion, then, the probability density function (PDF) of random quadratic form of interest is obtained, still in closed form. Therefore, false-alarm probability of the test can be reliably computed by means of a single numerical integration.

The work is articulated as follows: Sec. II develops the system model and the sensing scheme description. In Sec. III, the MGF and PDF of the test statistic are computed in closed-form for both settings of uncorrelated/correlated receiving sensors. The outcomes of our analytical derivation are contrasted with corresponding Monte Carlo simulated data in Section IV, where test performance with varying system parameters (e.g., number of collected samples, number of receive sensors, spatial correlation model and/or coefficient) is also reported. Sec. V concludes the work.

Notation: Throughout the paper, we denote vectors and matrices with boldface lowercase and uppercase letters, respectively. By $\mathrm{E}[\cdot]$ we denote the statistical expectation, while $\mathcal{U}(N)$, with positive integer N, stands for the unitary group of matrices of size N. $||\cdot||$ denotes the Euclidean norm of a vector, while by $\mathrm{tr}(\cdot)$ we denote the trace of a square matrix. For matrices and vectors, $(\cdot)^H$ indicates the conjugate-transpose. Finally, $|\cdot|$ is the determinant of a square matrix.

II. System Model and Spectrum Sensing Scheme

We focus on a SS setting, where a receiver equipped with K antennas collects N time samples from each antenna. We denote by $\mathbf{y}(n) = [y_1(n), \ldots, y_K(n)]^T$ the $K \times 1$ received vector at time $n \in \{1, \ldots, N\}$, with generic entry $y_k(n)$ denoting the discrete baseband complex sample at the k-th receive antenna.

Under $\mathcal{H}_0$, namely in absence of a primary signal, $y_k(n)$ is a vector of complex Gaussian noise samples with zero mean and variance σ_v^2

$$\mathbf{y}(n)|_{\mathcal{H}_0} = \mathbf{v}(n) \tag{1}$$

where $\mathbf{v}(n) \sim \mathcal{N}_{\mathbb{C}}(\mathbf{0}_{K\times 1}, \sigma_v^2 \mathbf{I}_{K\times K})$. Under $\mathcal{H}_1$, instead, both primary signal and noise are present, therefore

$$\mathbf{y}(n)|_{\mathcal{H}_1} = \mathbf{x}(n) + \mathbf{v}(n) = \mathbf{h}s(n) + \mathbf{v}(n) \tag{2}$$

where $s(n)$ is the transmitted signal sample, modeled without loss of generality as Gaussian distributed with zero mean and variance σ_s^2, while $\mathbf{h}$ is the $K \times 1$ unknown complex channel vector, affected by Rayleigh flat fading. The channel is assumed to be memoryless, and constant during the detection time, i.e., block fading is assumed. Under $\mathcal{H}_1$, we define the Signal-to-Noise Ratio (SNR) at the receiver as

$$\rho \triangleq \frac{\mathrm{E}\,\|\mathbf{x}(n)\|^2}{\mathrm{E}\,\|\mathbf{v}(n)\|^2} = \frac{\sigma_s^2}{\sigma_v^2}\frac{\|\mathbf{h}\|^2}{K}. \tag{3}$$

The detector collects the received samples in the $K \times N$ matrix

$$\mathbf{Y} \triangleq [\mathbf{y}(1) \ldots \mathbf{y}(N)] = \mathbf{h}\mathbf{s} + \mathbf{V} \tag{4}$$

where $\mathbf{s} \triangleq [s(1) \ldots s(N)]$ is a $1 \times N$ signal vector and $\mathbf{V} \triangleq [\mathbf{v}(1) \ldots \mathbf{v}(N)]$ is a $K \times N$ noise matrix. The sample covariance matrix $\mathbf{R}$ of the received samples is therefore given by

$$\mathbf{R} \triangleq \frac{1}{N}\mathbf{Y}\mathbf{Y}^H. \tag{5}$$

In our subsequent analysis, we shall make reference to the spectral decomposition of $\mathbf{R} = \mathbf{U}\mathbf{\Lambda}\mathbf{U}^H$, with $\mathbf{U}$ denoting the random unitary matrix of the eigenvectors, and $\mathbf{\Lambda}$ the diagonal matrix of the random eigenvalues, which are without loss of generality, denoted in non-increasing order as $\lambda_1 \geq \ldots \geq \lambda_K \geq 0$. The corresponding PDFs for $\mathbf{U}$ and $\mathbf{\Lambda}$ will be specified in Sec.III.

The test statistic employed by the detector to discriminate between the null hypothesis $\mathcal{H}_0$ and the presence of primary signal $\mathcal{H}_1$ is denoted by T; to take a decision, the detector compares it against a pre-defined threshold t: if $T > t$ it decides for $\mathcal{H}_1$, otherwise for $\mathcal{H}_0$. As a consequence, the *probability of false alarm* P_{fa} is defined as

$$P_{\mathrm{fa}} = \Pr(T > t|\mathcal{H}_0) \tag{6}$$

and the *probability of detection* P_d as

$$P_{\mathrm{d}} = \Pr(T > t|\mathcal{H}_1). \tag{7}$$

A. Sensing Scheme

The SS scheme we focus on, was introduced in [13]; such a method makes use of the sample eigenvector corresponding to the largest eigenvalue (i.e., λ_1) of (5) under $\mathcal{H}_1$, corresponding to the received sample matrix in (4), to heuristically improve the performance of RLRT [15] whose test statistic reads

$$T_{\mathrm{RLRT}} \triangleq \frac{\lambda_1}{\sigma_v^2}. \tag{8}$$

In fact, the EigenVEctor-aided (EVE) test assumes the availability of a set of M auxiliary signal slots, exploited to obtain the sample estimate of the eigenvector, say $\mathbf{u}_1$, corresponding to the largest eigenvalue λ_1. The decision is then made, based on a weighted mean of λ_1 with the energy contained in the leading eigenspace, in the mentioned M additional slots.

EVE test statistic is, therefore, expressed as

$$T_{\mathrm{EVE}} \triangleq \frac{\lambda_1 + M\mathbf{u}_1^H\mathbf{R}\mathbf{u}_1}{\sigma_v^2(M+1)}, \tag{9}$$

where M is the number of auxiliary slots exploited to estimate $\mathbf{R}$ under $\mathcal{H}_1$ and therefore to obtain the sample eigenvector estimate , corresponding to the largest eigenvalue . In absence of auxiliary data, T_{EVE} reduces to T_{RLRT}, whereas in presence of them, a performance gap in favor of T_{EVE} has been numerically observed (see [13], [14], and Fig.1). Clearly, as M grows, the effect of secondary data prevails upon the presence of the largest root λ_1 in the enumerator of (9). With this in mind, we postulate the availability of a sufficient number of secondary data to approximate T_{EVE} with a test where only the quadratic form at the enumerator is considered for SS purposes.

The resulting test, based on the statistics of the quadratic form

$$\mathbf{u}_1^H\mathbf{R}\mathbf{u}_1$$

at the enumerator of (9), will be hereinafter referred to as Quadratic Form Test (QFT), with statistic given by

$$T_{\mathrm{QFT}} \triangleq \frac{\mathbf{u}_1^H\mathbf{R}\mathbf{u}_1}{\sigma_v^2}, \tag{10}$$

and its analytical characterization under the null hypothesis will be the core of the present work.

III. Statistical Characterization of the Test

QFT statistic (10) can be rewritten, in terms of the spectral decomposition of $\mathbf{R}$, as

$$W = \frac{\mathbf{u}_1^H\mathbf{U}\mathbf{\Lambda}\mathbf{U}^H\mathbf{u}_1}{N\sigma_v^2},$$

where we recall that $\mathbf{U} \in \mathcal{U}(K)$, and $\mathbf{\Lambda}$ is a positive-definite matrix with probability 1. The MGF of W can be written as

$$\Phi_W(s) = \mathrm{E}[e^{-sW}] = \mathrm{E}\left[\exp\left(-\mathrm{tr}\left(s\frac{\mathbf{u}_1\mathbf{u}_1^H\mathbf{U}\mathbf{\Lambda}\mathbf{U}^H}{N\sigma_v^2}\right)\right)\right], \tag{11}$$

$$f_W(t) = C_{\mathcal{M}} \sum_{j=1}^{K} \frac{\kappa_j (N\sigma_v^2)^{N-j+1}(N-j)! t^{N+K-j-1}}{(N+K-j-1)!} \exp\left(-tN\sigma_v^2\right) {}_1F_1\left(K-1; N+K-j; N\sigma_v^2 t\right),\ t>0, \tag{12}$$

where the expectation is to be taken jointly w.r.t. both $\mathbf{U}$ and $\mathbf{\Lambda}$.

Since the probability density of $\mathbf{R}$ assumes different expressions and properties depending on whether correlation is present among the K receiving sensors, we first compute the average for the uncorrelated case in the following Proposition, secondly, we provide the analysis for the correlated case, and we refer the reader to Sec.IV for explicit instances of the mentioned correlation.

Proposition III.1. *In absence of correlation among receiving sensors, the MGF of the quadratic form of interest assumes the following expression:*

$$\Phi_W(s) = C_{\mathcal{M}} \frac{|\mathbf{G}(s)|}{s^{K-1}}, \tag{13}$$

with $K \times K$ matrix $\mathbf{G}(s)$ having entries

$$[\mathbf{G}(s)]_{i,j} = \begin{cases} \frac{(N-j)!}{(1+\frac{s}{N\sigma_v^2})^{N-j+1}},\ i=1,\ j=1,\dots,K \\ (N+K-i-j)!\, i=2,\dots,K,\ j=1,\dots,K \end{cases}$$

while

$$C_{\mathcal{M}} = \frac{(-N\sigma_v^2)^{K-1}(K-1)!}{\prod_{\ell=1}^{K}(K-\ell)!(N-\ell)!}.$$

Proof. In absence of spatial correlation, $\mathbf{R}$ under $\mathcal{H}_0$ can be suitably modelled by a complex central uncorrelated Wishart matrix, of size K and with $N \geq K$ degrees of freedom, with density

$$p(\mathbf{R}) = \frac{|\mathbf{R}|^{N-K} e^{-\mathrm{tr}(\mathbf{R})}}{\prod_{\ell=1}^{K}(\sqrt{\pi})^{K-1}(N-\ell)!}. \tag{14}$$

To compute the expectation in (11), (14) should be transformed exploiting the Jacobian of eigenvalue-eigenvector decomposition for $\mathbf{R} = \mathbf{U}\mathbf{\Lambda}\mathbf{U}^H$ (see [22, Eq. (6)] and [21, Eq. (6)]) leading to

$$p(\mathbf{R})\, d\mathbf{R} = \frac{\prod_{\ell=1}^{K} \lambda_\ell^{N-K} e^{-\lambda_\ell} \prod_{i<j}(\lambda_i - \lambda_j)^2}{\prod_{\ell=1}^{K}(K-\ell)!(N-\ell)!} d\mathbf{\Lambda} d\mathbf{U}. \tag{15}$$

Notice that (15), to be plug into (11) to compute the average, does not depend on $\mathbf{U}$. Therefore, the integral over the unitary group reduces to the following instance of Harish-Chandra–Itzykson-Zuber (HCIZ) integral [18, Eq. (92)]

$$\int_{\mathcal{U}(K)} \exp\left\{-\mathrm{tr}\left(\frac{s}{N\sigma_v^2}\mathbf{u}_1\mathbf{u}_1^H \mathbf{U}\mathbf{\Lambda}\mathbf{U}^H\right)\right\} d\mathbf{U} = {}_0F_0\left(-\frac{s}{N\sigma_v^2}\mathbf{u}_1\mathbf{u}_1^H, \mathbf{\Lambda}\right), \tag{16}$$

with ${}_0F_0(\cdot,\cdot)$ the hypergeometric function of two matrix arguments (see e.g., [24, Eq. (9)]), one of which being the rank-one matrix $-\frac{s}{N\sigma_v^2}\mathbf{u}_1\mathbf{u}_1^H$ of size K, whose unique non-zero eigenvalue is given by $-\frac{s}{N\sigma_v^2}$. A determinantal expression for the mentioned hypergeometric function is available in [24, Corollary I]; particularizing it to our case, we get

$${}_0F_0\left(-\frac{s}{N\sigma_v^2}\mathbf{u}_1\mathbf{u}_1^H, \mathbf{\Lambda}\right) = \frac{(K-1)!\,|\mathbf{\Theta}(s)|}{(-\frac{s}{N\sigma_v^2})^{K-1}\prod_{i<j}(\lambda_i-\lambda_j)}, \tag{17}$$

with the $K \times K$ matrix $\mathbf{\Theta}(s)$ having entries

$$[\mathbf{\Theta}(s)]_{i,j} = \begin{cases} \exp\left(-\frac{s}{N\sigma_v^2}\lambda_i\right), & i=1,\dots,K,\ j=1, \\ \lambda_i^{K-j} & i=1,\dots,K,\ j=2,\dots,K. \end{cases}$$

The last step of the computation requires an integral over $\mathbf{\Lambda}$, which can be performed w.r.t. the set of unordered eigenvalues as well, due to the fact that the integrands are symmetric functions of the whole set of eigenvalues of $\mathbf{R}$. This is tantamount to solve, with the help of [21, Corollary I] and of [19, 3.351],

$$\frac{1}{K!}\int_{(0,+\infty)^K} |\mathbf{\Theta}(s)| \prod_{i<j}(\lambda_i-\lambda_j)^2 \times \prod_{\ell=1}^{K} \lambda_\ell^{N-K} e^{-\lambda_\ell} d\lambda_\ell = |\mathbf{G}(s)| \tag{18}$$

from which, upon proper simplifications of the normalizing constant, we obtain (13).

□

Upon Laplace inversion of (13), the PDF of W is retrieved, with the expression showed in (12) with ${}_1F_1(a;b;z)$ being the Confluent Hypergeometric Function [20, Ch.13], and κ_j the co-factor of the $(1,j)$-th entry of $\mathbf{G}(s)$ in Proposition III.1.

A similar expression holds for the MGF of a quadratic form obtained in a case of correlated samples. The derivation is, however, made more involved by the fact that, in the correlated case, the PDF of $\mathbf{R}$ depends on both its eigenvalues as well as on its eigenvectors. This circumstance does not prevent us from obtaining a closed-form expression for the MGF; however, from the exact expression it is not possible to obtain an explicit expression for the PDF of W. We resort, therefore, to an approximation, sustained by numerical evidence, as shown in Section IV.

Proposition III.2. *Whenever the received samples, collected by the K-antenna equipped sensing array, are spatially correlated, a suitable approximation for the MGF of W is:*

$$\widetilde{\Phi}_W(s) = C_{\mathbf{\Sigma}} \frac{|\mathbf{T}(s)|}{s^{K-1}}, \tag{19}$$

with $\mathbf{T}(s)$ *having entries*

$$[\mathbf{T}(s)]_{i,j} = \begin{cases} \dfrac{(N-K)!}{\left(\frac{1}{\sigma_i} + \frac{s}{N\sigma_v^2}\right)^{N-K+1}}, \; i = 1, \ldots, K, j = 1, \\ (N-j)!\sigma_i^{N-j+1}, \; i = 1, \ldots, K, j = 2, \ldots, K, \end{cases}$$

while

$$C_{\mathbf{\Sigma}} = \frac{(-N\sigma_v^2)^{K-1}(K-1)!}{\prod_{\ell=1}^{K} \sigma_\ell^{N-K+1}(N-\ell)! \prod_{i<j}(\sigma_i - \sigma_j)}.$$

Above, the positive-definite square matrix $\mathbf{\Sigma}$ *of size* K *represents the correlation of the sample covariance matrix* $\mathbf{R}$*, with distinct, ordered eigenvalues denoted by* $\sigma_1 > \ldots > \sigma_K > 0$*'s.*

Proof. In a correlated scenario, $\mathbf{R}$ follows a complex central correlated Wishart distribution, with N degrees of freedom and correlation matrix $\mathbf{\Sigma}$ [18, Eq.(94)]

$$p(\mathbf{R}) = \frac{|\mathbf{R}|^{N-K} e^{-\mathrm{tr}(\mathbf{\Sigma}^{-1}\mathbf{R})}}{|\mathbf{\Sigma}|^N \prod_{\ell=1}^{K} (\sqrt{\pi})^{K-1}(N-\ell)!}. \tag{20}$$

Upon spectral decomposition, (20) reads as

$$p(\mathbf{R})\, d\mathbf{R} = \frac{|\mathbf{\Lambda}| e^{-\mathrm{tr}(\mathbf{\Sigma}^{-1}\mathbf{U}\mathbf{\Lambda}\mathbf{U}^H)} \prod_{i<j}(\lambda_i - \lambda_j)^2}{\prod_{\ell=1}^{K} \sigma_\ell^N (K-\ell)!(N-\ell)!} d\mathbf{\Lambda} d\mathbf{U}. \tag{21}$$

Plugging (21) into (11), again with the help of HCIZ integral, a closed-form expression is retrieved for the MGF of W, namely

$$\widetilde{\Phi}_W(s) = \frac{s^{1-K} |\mathbf{F}(s)| |\mathbf{\Sigma}|^{-N}}{\prod_{\ell=1}^{K}(K-\ell)!(N-\ell)! \prod_{i<j}(\omega_i(s) - \omega_j(s))}, \tag{22}$$

with $\omega_1(s), \ldots, \omega_K(s)$ the eigenvalues of the matrix

$$\mathbf{\Sigma}^{-1} + \frac{s}{N\sigma_v^2} \mathbf{u}_1 \mathbf{u}_1^H,$$

and with $\mathbf{F}(s)$ having entries

$$[\mathbf{F}(s)]_{i,j} = \frac{(N-j)!}{\omega_i(s)^{N-j+1}}, \; i, j = 1, \ldots, K.$$

Unfortunately to our goals, the dependence of (22) on the variable s makes it non amenable to Laplace inversion. For this reason, we adopt an approximation, and carry over our computation by neglecting the dependence of (20) on $\mathbf{U}$. Specifically, we plug the joint density of the ordered eigenvalues of a correlated Wishart matrix [21, Eq. (17)] into (11); we then exploit HCIZ integral as in (16), and we finally obtain, performing the average w.r.t. $\mathbf{\Lambda}$ still with the help of [21, Corollary I], the expression in (19).

Such an expression, albeit based on an approximation, matches with simulated data, as extensively discussed in next Section. □

The corresponding PDF can be expressed as

$$f_W(t) = \widetilde{C_{\mathbf{\Sigma}}} \sum_{i=1}^{K} \frac{\kappa_i t^{N-1}}{\exp\left(\frac{tN\sigma_v^2}{\sigma_i}\right)} {}_1F_1\left(K-1; N; \frac{tN\sigma_v^2}{\sigma_i}\right), \tag{23}$$

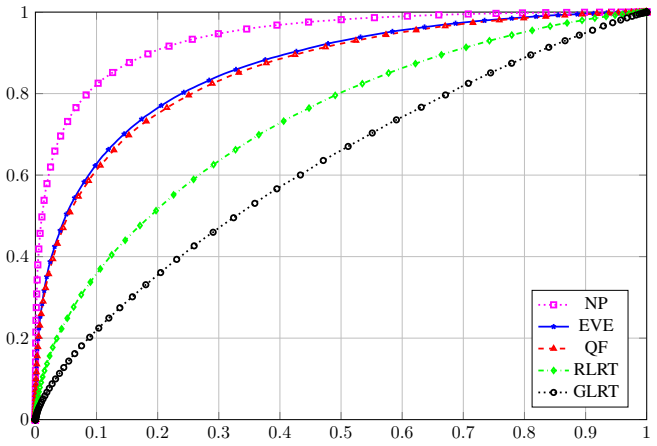

Fig. 1. ROC curve, $N = 64$, $K = 8$, $M = 4$ for EVE and QFT, SNR $= -5$ dB.

for $t > 0$ and with

$$\widetilde{C_{\mathbf{\Sigma}}} = \frac{(-1)^{K-1}(N\sigma_v^2)^N (K-1)!}{(N-1)!|\mathbf{\Sigma}|^{N-K+1} \prod_{i<j}(\sigma_i - \sigma_j) \prod_{\ell=1}^{K-1}(N-\ell)!}.$$

Remark I The extension of Proposition III.2 to the case of non-distinct eigenvalues is possible, by exploiting tools provided in [24, Lemma 3].

IV. Numerical Results

The rationale behind our work is the capability of EVE test (9) to outperform other widely adopted SS strategies. Numerical evidence thereof is reported in Fig. 1, where the Receive Operating Characteristic (ROC) curve is shown for EVE, QFT and RLRT, GLRT and the Neyman-Pearson reference test. For the sake of clarity, we recall that the GLRT test statistic is given by [12]

$$T_{\mathrm{GLRT}} = \frac{\lambda_1}{\frac{1}{K}\mathrm{tr}(\mathbf{R})}, \tag{24}$$

while the Neyman-Pearson test, which requires the exact knowledge of both channel vector $\mathbf{h}$ and noise variance σ_v^2, under the assumption of independent Gaussian samples, is given by [12]

$$T_{\mathrm{NP}} = \frac{\left(\pi\sigma_v^2\right)^{NK} \exp\left(-N\mathrm{tr}(\mathbf{R}\mathbf{\Gamma}^{-1})\right)}{\left(\pi^K |\mathbf{\Gamma}|\right)^N \exp\left(-\frac{N\mathrm{tr}(\mathbf{R})}{\sigma_v^2}\right)} \tag{25}$$

where $\mathbf{\Gamma} = \sigma_v^2 \mathbf{I}_{K\times K} + \sigma_s^2 \mathbf{h}\mathbf{h}^H$. For EVE and QFT, $M = 4$ auxiliary slots have been used for the estimation of the sample eigenvector $\mathbf{u}_1$. To corroborate the motivation of our analytical study, it is evident how the performance of QFT almost matches EVE one's with very few auxiliary slots. Fig. 2 shows instead the performance curve, i.e., P_d as a function of the SNR, with target $P_{fa} = 0.01$.

Analytical are compared against simulated data in Fig. 3. The empirical PDFs have been generated by means of extensive Monte Carlo simulation, with 10^6 iterations and 1000 bins

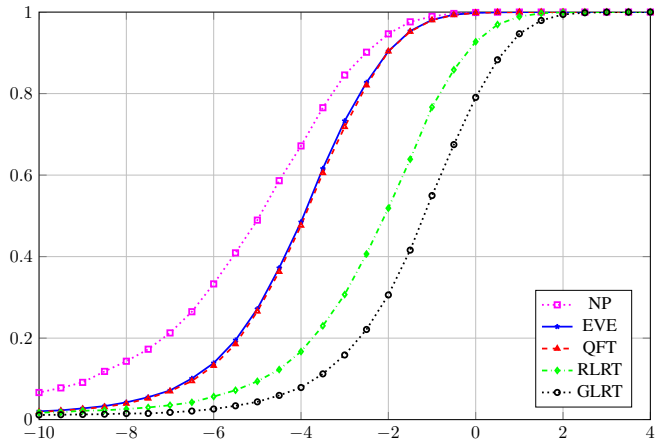

Fig. 2. Performance curve, P_d vs. SNR, $N = 64$, $K = 8$, $M = 4$ for EVE and QFT, $P_{fa} = 0.01$.

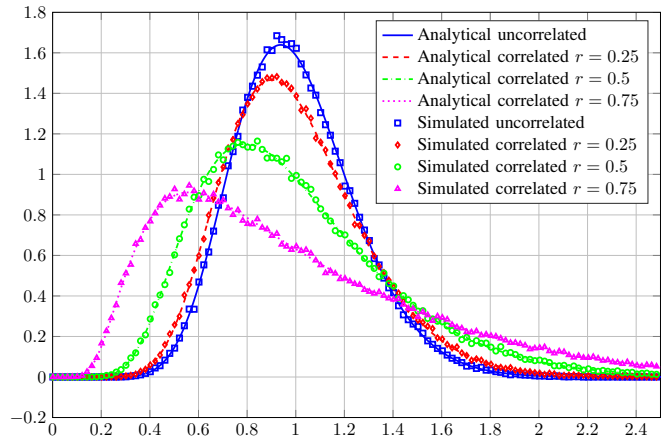

Fig. 3. PDF of QFT, analytical vs. simulated, $N = 16$, $K = 4$.

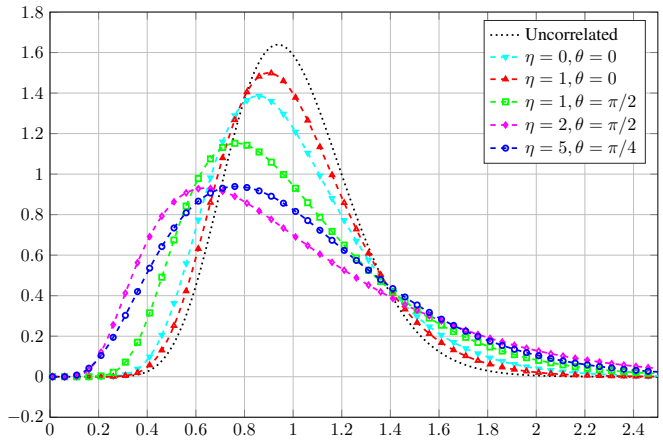

Fig. 4. PDF of QFT with nonisotropic scattering correlation model, $N = 16$, $K = 4$.

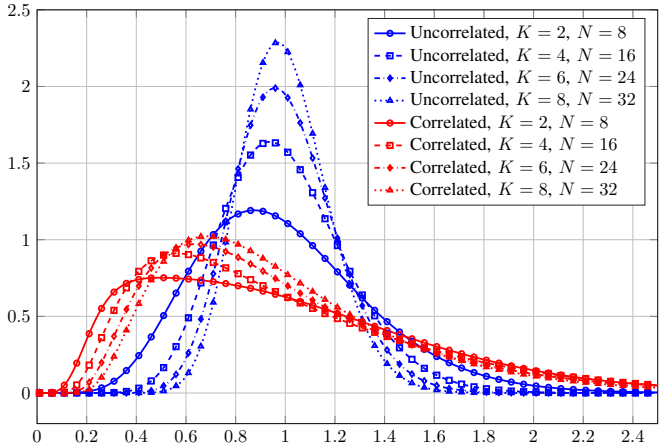

Fig. 5. PDF of QFT with uncorrelated and exponentially correlated model ($r = 0.75$) for varying K and N.

per histogram. It can be noticed that theoretical and empirical PDFs almost perfectly match by following expressions (12) and (23), for fixed number of receive sensors $K = 4$ and collected samples $N = 16$. Color-coded curves refer to an uncorrelated setting, and to an exponentially-correlated (see [21, Sec.VI-A]) model, with varying values of the correlation coefficient, and spatial correlation matrix having (i, j)-th entry

$$[\mathbf{\Sigma}]_{i,j} = r^{|i-j|}, \qquad r \in [0, 1) \tag{26}$$

In (26), r represents the correlation coefficient between consecutive sensors, assuming a linear array placement. As expected, the PDF of W shifts toward the left as the spatial correlation between receiving antenna increases.

A different model of spatial correlation, proposed in [25], due to its capabilities of accounting for non-isotropic scattering conditions, is adopted in Fig. 4, with corresponding expression of the correlation matrix elements given by

$$[\mathbf{\Sigma}]_{i,j} = \frac{I_0\left(\sqrt{\eta^2 - 4\pi d_{i,j}^2 + j4\pi\eta\sin(\theta)d_{i,j}}\right)}{I_0(\eta)}. \tag{27}$$

In (27), $d_{i,j}$ represents the distance between sensor i and sensor j at the receiver; η is a tuning parameter for the degree of anisotropy of scattering [21], [25], set to 0 for isotropic settings, and whose value increases with increasing directionality of the scattering. Finally, $\theta \in [0, \pi/2]$ represents the average direction of the angle of arrival on the receiving array. The PDFs of both correlation models have the same numbers of receiving sensors $K = 4$ and collected samples $N = 16$. With (12) as a reference, we notice that, for fixed mean angle of arrival direction $\theta = \pi/2$, the degree of anisotropy plays a major role in received energy degradation (see the gap between the curves corresponding to $\eta = 1$ and $\eta = 2$ for given θ), whereas when $\theta = 0$ a narrower angle of arrival helps energy collection. In Figure 5, to conclude our investigation, we focus on the impact of the number of sensors and samples on the performance of the test, contrasting the shape in the uncorrelated case, getting narrower and more peaked as both N and K increase, while the same effect is achieved much more slowly in a strongly correlated case

(model (26) with $r = 0.75$), when the same number of samples and sensors are collected and, respectively, deployed. For fairness of comparison, we keep the ratio K/N constant across the curves depicted in the figure.

V. Conclusion

The test statistic of a SS algorithm based on a random quadratic form, with kernel matrix given by the covariance of the collected time samples, has been studied under the null hypothesis (absence of primary signal). A MGF-based approach has been carried out for different settings, enhancing the risk of performance loss caused by the presence of spatial correlation between receiving sensors. This analytical study paves the way to a more refined characterization of the EVE test, jointly exploiting the largest eigenvalue and a sample estimate of its corresponding eigenvector, currently under investigation. Also, the analytical framework adopted in this paper can suitably model a scenario where the same SS algorithm is exploited in presence of an Intelligent Reflecting Surface, meant to aid primary user communication only. Such an extension will be the subject of future works.

Acknowledgment

The work of Daniel Gaetano Riviello was partially supported by the European Union – NextGenerationEU – National Recovery and Resilience Plan (Piano Nazionale di Ripresa e Resilienza, PNRR) through the Project: "SoBigData.it – Strengthening the Italian RI for Social Mining and Big Data Analytics", under Grant Prot. IR0000013 – Avviso n. 3264 del 28/12/2021.

The work of Giusi Alfano and Roberto Garello was partially supported by the European Union - Next Generation EU under the Italian National Recovery and Resilience Plan (NRRP), Mission 4, Component 2, Investment 1.3, CUP E13C22001870001, partnership on "Telecommunications of the Future" (PE00000001 - program "RESTART").

References

[1] F. Tariq, *et al.*, "A speculative study on 6G," *IEEE Trans. Wireless Commun.* , vol. 27, no. 4, pp. 118–125, Aug. 2020.

[2] W. Jiang, B. Han, M. A. Habibi, and Hans D. Schotten, "The road towards 6G: A comprehensive survey," *IEEE Open J. Commun. Soc.*, vol. 2, pp. 334–366, Feb. 2021.

[3] M. R. Dakkak, D.G. Riviello, A. Guidotti, and A. Vanelli-Coralli "Evaluation of multi-user multiple-input multiple-output digital beamforming algorithms in B5G/6G low Earth orbit satellite systems", *Int. J. Satell. Commun. Network.*, pp. 1–17, Aug. 2023.

[4] A. Ivanov, K. Tonchev, V. Poulkov, and A. Manolova, "Probabilistic spectrum sensing based on feature detection for 6G cognitive radio: a survey," *IEEE Access*, vol. 9, pp. 116994–117026, Aug. 2021.

[5] A. Kortun, T. Ratnarajah, M. Sellathurai, C. Zhong, and C. B. Papadias, "On the performance of eigenvalue-based cooperative spectrum sensing for cognitive radio," *IEEE J. Sel. Topics Signal Process.*, vol. 5, no. 1, pp. 49–55, Feb. 2011.

[6] P. Salvo Rossi, D. Ciuonzo, and G. Romano, "Orthogonality and Cooperation in Collaborative Spectrum Sensing through MIMO Decision Fusion," *IEEE Trans. Wireless Commun.* , vol. 12, no. 11, pp. 118–125, Nov. 2013.

[7] Y. Li, W. Zhang, C.-X. Wang, J. Sun, and Y. Liu, "Deep reinforcement learning for dynamic spectrum sensing and aggregation in multi-channel wireless networks," *IEEE Trans. Cog. Comm. and Net.* , vol. 6, no. 2, pp. 464–475, June 2020.

[8] F. Penna, R. Garello, and M. A. Spirito, "Cooperative Spectrum Sensing based on the Limiting Eigenvalue Ratio Distribution in Wishart Matrices," *IEEE Comm. Letters*, vol.13, no.7, pp.507–509, July 2009.

[9] F. Penna, R. Garello and M. A. Spirito, "Probability of Missed Detection in Eigenvalue Ratio Spectrum Sensing," *2009 IEEE Int. Conf. on Wireless and Mobile Computing, Networking and Communications*, Marrakech, Morocco, 2009, pp. 117–122.

[10] L. Wei, and O. Trikkonenn, "Spectrum Sensing in the Presence of Multiple Primary Users," *IEEE Trans. on Comm.* , vol. 60, no. 5, pp.1268–1277, Mar. 2012.

[11] M. F. Arts, *Eigenvalue-Based Spectrum Sensing for Cognitive Radio,* RWTH Aachen Phd Thesis, 2017.

[12] P. Bianchi, M. Debbah, M. Maïda, and J. Najim "Performance of Statistical Tests for Source Detection using Random Matrix Theory," *IEEE Trans. Inf. Theory*, vol. 57, no. 4, pp. 2400–2419, Apr. 2011.

[13] R. Garello, and Y. Jia, "Improving Spectrum Sensing Performance by using Eigenvectors," *Proc. 1st Int'l Conf. on Advances in Cognitive Radio (COCORA) 2011*, Budapest, Hungary, pp.25–30, Apr. 2011.

[14] D.G. Riviello, P. Dakhal, and R. Garello, "Performance Analysis of Multi-Antenna Hybrid Detectors and Optimization with Noise Variance Estimation", *Proc. 2nd Int'l Conference on Sig. Proc. Int. Net. (SPIN) 2015*, Dehli, India, pp.44–49, Feb. 2015.

[15] S. N. Roy, "On a heuristic method of test construction and its use in multivariate analysis", *Ann. Math. Stat.*, vol. 24, no. 2, pp. 220–238, 1953.

[16] P. Dhakal, S. K. Sharma, S. Chatzinotas, B. Ottersten, and D. Riviello, "Effect of primary user traffic on largest eigenvalue based spectrum sensing technique," *Proc. 11th Int. Conf. (CROWNCOM)*, Grenoble, France, pp. 67–78, May 2016.

[17] F. Penna, and R. Garello, "Decentralized Neyman-Pearson Test with Belief Propagation for Peer-to-Peer Collaborative Spectrum Sensing," in *IEEE Trans. on Wireless Commun.*, vol. 11, no. 5, pp. 1881–1891, May 2012.

[18] A. T. James, "Distribution of matrix variates and latent roots derived from normal samples," *Ann. Math. Stat.,* vol. 35, no. 2, pp. 474–501, June 1964.

[19] I. S. Gradshteyn, and I. M. Ryzhik, *Table of integrals, series, and products*, Academic Press, New York, 1980.

[20] M. Abramowitz, I. Stegun, *Handbook of Mathematical Functions*, National Bureau of Standards, Washington, 1964.

[21] M. Chiani, M.Z. Win, and A. Zanella, "On the capacity of spatially correlated MIMO Rayleigh-fading channels," *IEEE Trans. Inf. Theory*, vol. 49, no. 10, pp. 2363–2371, Oct. 2003.

[22] P. Dharmawansa, P. Dissanayakeand, and Y. Chen, "The eigenvectors of single-spiked complex Wishart matrices: finite and asymptotic analyses",*IEEE Trans. Inf. Theory*, vol. 68, no. 12, pp. 8092–8120, 2022.

[23] A. Zanella, and M. Chiani, "On the distribution of the ℓ-th largest eigenvalue of complex Wishart matrices," *Acta Physica Polonica B*, vol. 51, no. 7, 2020.

[24] M. Chiani, M.Z. Win, and H. Shin, "MIMO Networks: the Effects of Interference," *IEEE Trans. Inf. Theory*, vol. 56, no. 1, pp. 336–349, Jan. 2010.

[25] A. Abdi, and M. Kaveh, "A space-time correlation model for multielement antenna systems in mobile fading channels," *IEEE J. Select. Areas Commun.*, vol. 20, pp. 550–560, Apr. 2002.